Supporting Information for

An 1,3,4-oxadiazole-based OFF-ON fluorescent chemosensor for Zn^{2+} in aqueous solution and imaging application in living cells

Ji-An Zhou,[a] Xiao-Liang Tang,[a] Ju Cheng,[b] Zheng-Hua Ju,[a] Li-Zi Yang,[a] Wei-Sheng Liu,*[a] Chun-Yang Chen[a] and De-Cheng Bai[b]

[a] *Key Laboratory of Nonferrous Metal Chemistry and Resources Utilization of Gansu Province and State Key Laboratory of Applied Organic Chemistry, College of Chemistry and Chemical Engineering, Lanzhou University, Lanzhou, 730000, P. R. China. E-mail: liuws@lzu.edu.cn; Fax: +86-931-8912582; Tel: +86-931-8915151*

[b] *School of Basic Medical Sciences, Lanzhou University, Lanzhou, 730000, P. R. China*

Table of contents

1. **Determination of the association constant of 1-Zn^{2+} system in acetonitrile. (*Fig. S1-S2*)**
2. **Fluorescence and absorption titration of 1 with Cd^{2+} in acetonitrile. (*Fig. S3-S5*)**
3. **Fluorescence and absorption titration of 1 with Mg^{2+} in acetonitrile. (*Fig. S6-S8*)**
4. **Effect of water content on the fluorescence response of 1 and its complexes. (*Fig. S9-S10*)**
5. **Absorption titration of 1 with Zn^{2+}, Cd^{2+} and Mg^{2+} in 1:1 CH_3CN/H_2O. (*Fig. S11*)**
6. **Effect of the pH on the fluorescence intensity of 1 and 1-Zn^{2+} in CH_3CN-H_2O mixed solvent. (*Fig. S12*)**
7. **The detection limit (LOD) and association constant of 1-Zn^{2+} in HEPES buffer. (*Fig. S13*)**
8. **Photo showing in natural light and fluorescence changes. (*Fig. S14*)**
9. **Time-resolved fluorescence decay, radiative rate and nonradiative rate data. (*Table. S1*)**
10. **Theoretical modeling. (*Table. S2*)**
11. **^1H NMR, ^{13}C NMR and ESI-MS spectra of 1 and 2 in $CDCl_3$ (*Figure S15-S20)***

1. Determination of the association constant of 1-Zn^{2+} complex system.

The total binding constant of **1** complexing with Zn^{2+} was studied by the absorbance curve at 364 nm, which was obtained from the absorbance titration spectra of **1** with the increase of $Zn(ClO_4)_2$ in acetonitrile solution. Job's plot analysis of the fluorescence and the absorbance titration for **1**-Zn^{2+} system both exhibited 1:1 stoichiometry. The equilibrium is given by following equation:

$$\mathrm{M} + \mathrm{L} \leftrightarrow \mathrm{ML}$$

The association constant, *K*, is expressed as:

$$K = \frac{[\mathrm{ML}]}{[\mathrm{M}]_{\mathrm{eq}}[\mathrm{L}]_{\mathrm{eq}}} = \frac{[\mathrm{ML}]}{([\mathrm{M}]-[\mathrm{ML}])(\mathrm{c_L}-[\mathrm{ML}])}$$

where $[M]_{eq}$, $[L]_{eq}$ and [ML] are the equilibrium concentrations of free Zn^{2+}, ligand **1** and **1**-Zn^{2+}, respectively. [M] and c_L are the initial concentrations of Zn^{2+} and ligand **1**, respectively. The equation is transformed to:

$$[\mathrm{ML}] = \frac{(\mathrm{c_L} + [\mathrm{M}] + 1/\mathrm{K}) - \sqrt{(\mathrm{c_L} + [\mathrm{M}] + 1/\mathrm{K})^2 - 4 \times \mathrm{c_L} \times [\mathrm{M}]}}{2}$$

Absorbance is given by the Lambert-Beer law as follows:

$$A_0 = \varepsilon_0 \mathrm{c_L} l$$

$$A = \varepsilon_0 [\mathrm{L}]_{\mathrm{eq}} l + \varepsilon [\mathrm{ML}] l$$

$$A_{\mathrm{max}} = \varepsilon [\mathrm{ML}]_{\mathrm{max}} l = \varepsilon \mathrm{c_L} l$$

A_0 is the absorbance of **1** at 364 nm without Zn^{2+}, A is the absorbance of **1** at 364 nm obtained with Zn^{2+}, and A_{max} is the absorbance of **1** at 364 nm in the presence of excess amount of Zn^{2+}. These relations together with $c_L = [L]_{eq} + [ML]$ lead to:

$$\frac{A - A_0}{A_{\mathrm{max}} - A_0} = \frac{[\mathrm{ML}]}{\mathrm{c_L}}$$

Thus, the following equation is obtained:

$$A = A_0 + \frac{A_{\mathrm{max}} - A_0}{2}\left\{\left(1 + \frac{[\mathrm{M}]}{\mathrm{c_L}} + \frac{1}{\mathrm{c_L K}}\right) - \sqrt{\left(1 + \frac{[\mathrm{M}]}{\mathrm{c_L}} + \frac{1}{\mathrm{c_L K}}\right)^2 - 4 \times \frac{[\mathrm{M}]}{\mathrm{c_L}}}\right\}$$

The equation was used for fitting of the absorption titration data with Zn^{2+}. The obtained curve is shown in Figure S1.

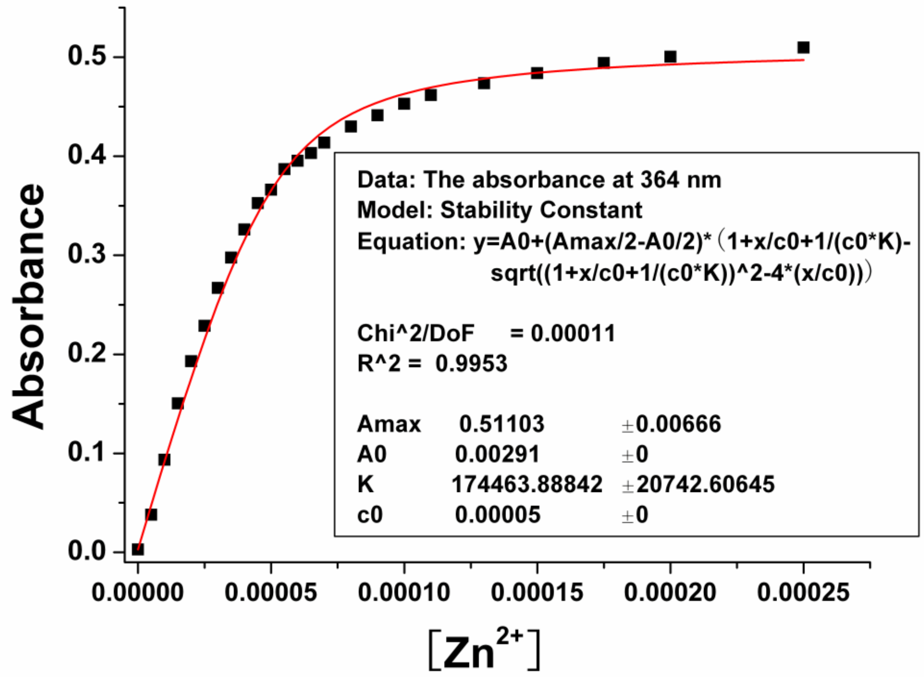

Fig. S1 The absorbance change of **1** at 364 nm in acetonitrile with the increase of $Zn(ClO_4)_2$. The red line is the nonlinear fitting curve obtained assuming a 1:1 association between **1** and Zn^{2+}. [**1**] = 5.0×10^{-5} M.

The same equation was used for fitting of the fluorescence data by fluorescence titration for **1**-Zn^{2+} system:

$$F = F_0 + \frac{F_{\max} - F_0}{2}\{(1 + \frac{[\mathrm{M}]}{\mathrm{c_L}} + \frac{1}{\mathrm{c_L K}}) - \sqrt{(1 + \frac{[\mathrm{M}]}{\mathrm{c_L}} + \frac{1}{\mathrm{c_L K}})^2 - 4 \times \frac{[\mathrm{M}]}{\mathrm{c_L}}}\}$$

F_0 is the fluorescence intensity of **1** at 439 nm without Zn^{2+}, F is the fluorescence intensity of **1** at 439 nm obtained with Zn^{2+}, and $F_{\max}$ is the fluorescence intensity of **1** at 439 nm in the presence of excess amount of Zn^{2+}. The obtained curve is shown in Figure S2.

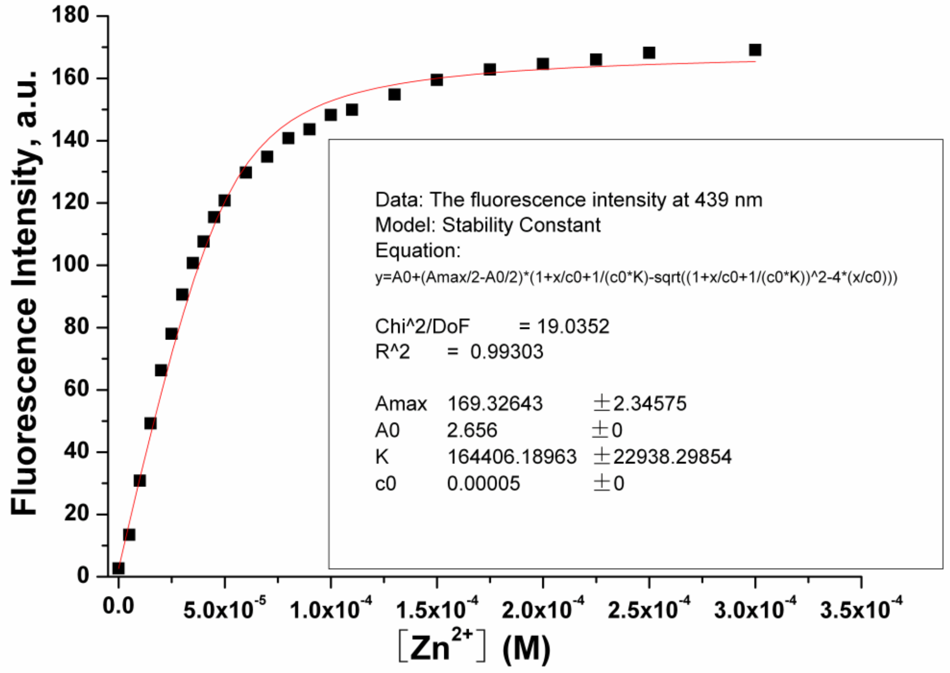

Fig. S2 Change in the fluorescence intensity at 439 nm. The red line is the nonlinear fitting curve obtained assuming a 1:1 association between **1** and Zn^{2+}. The association constant was estimated to be 1.6 (± 0.2) × 10^5 M^{-1}. [**1**] = 5.0 × 10^{-5} M, λ_{ex} = 333 nm.

2. Fluorescence and absorption titration of 1 with Cd^{2+} in acetonitrile.

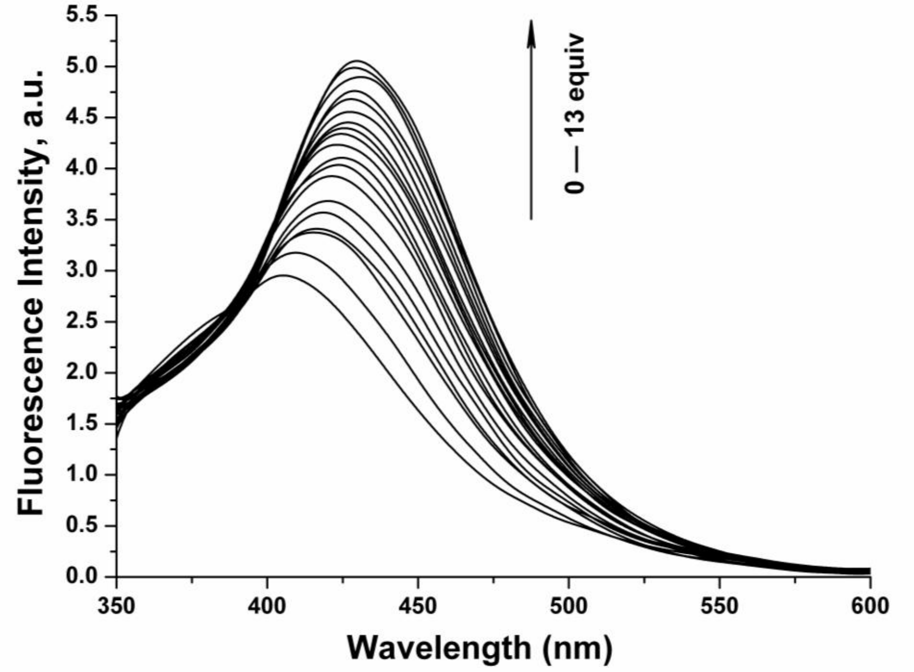

Fig. S3 Fluorescence spectra of **1** in acetonitrile in the presence of increasing concentration of $Cd(ClO_4)_2$. λ_{ex} = 333 nm, [**1**] = 5.0×10^{-5} M.

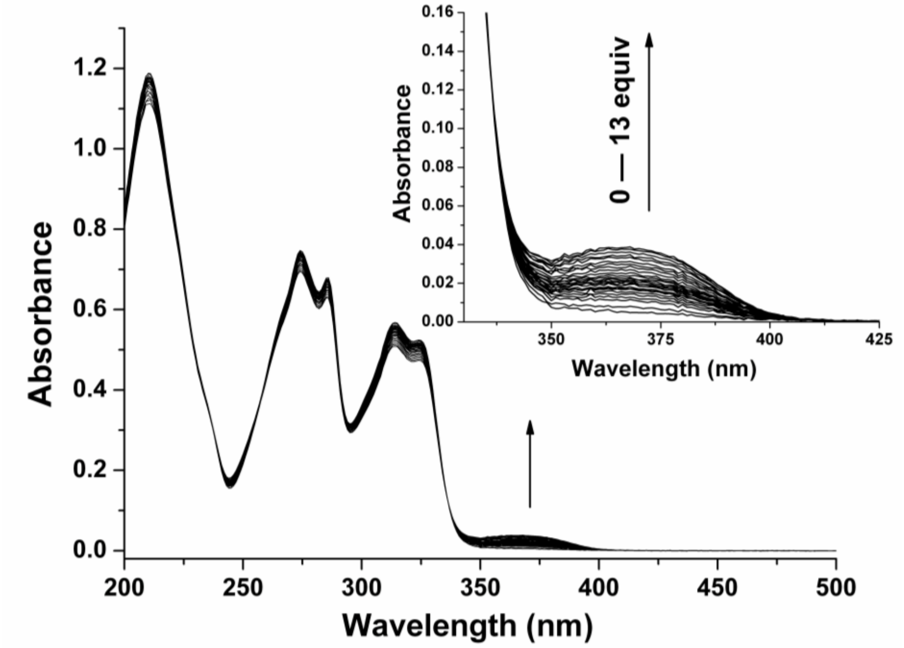

Fig. S4 Absorption spectra of **1** in acetonitrile with the increase of $Cd(ClO_4)_2$. Inset: The absorbance change of **1** at 367 nm. [**1**] = 5.0×10^{-5} M.

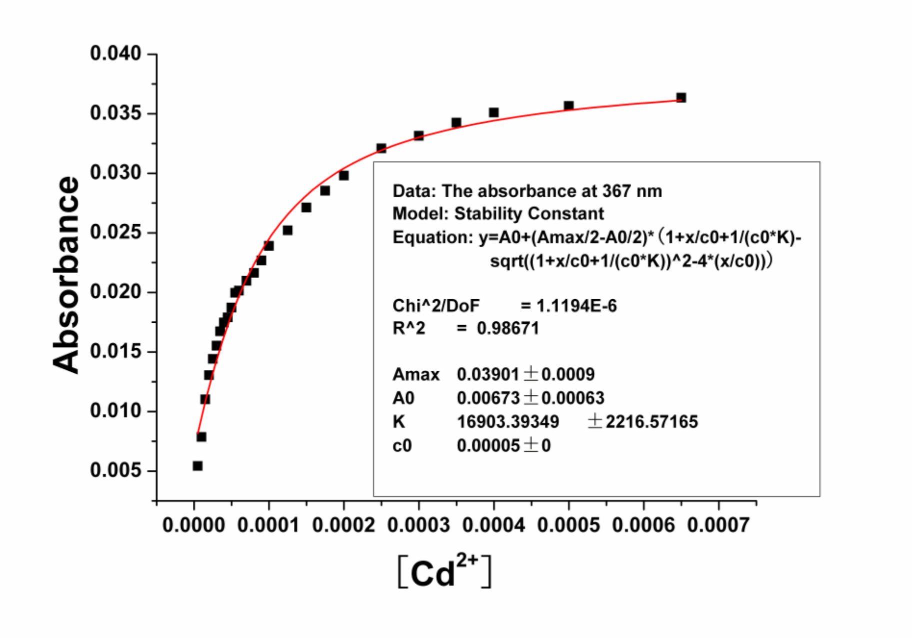

Fig. S5 The absorbance change of **1** at 367 nm in acetonitrile with the increase of $Cd(ClO_4)_2$. The red line is the nonlinear fitting curve obtained assuming a 1:1 association between **1** and Cd^{2+}. The association constant was estimated to be 1.7 (± 0.2) × 10^4 M^{-1}. [**1**] = 5.0 × 10^{-5} M.

3. Fluorescence and absorption titration of 1 with Mg^{2+} in acetonitrile.

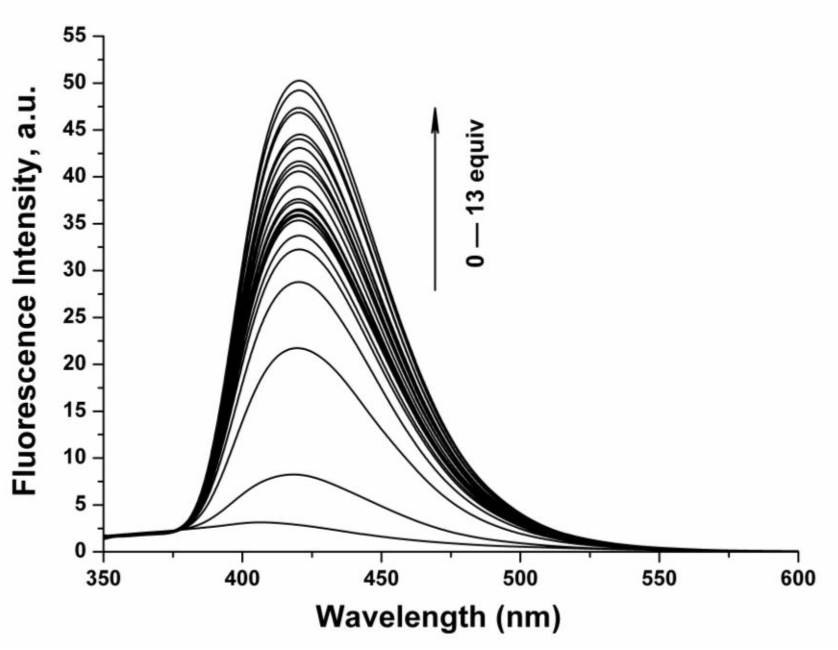

Fig. S6 Fluorescence spectra of **1** in acetonitrile in the presence of increasing concentration of $Mg(ClO_4)_2$. λ_{ex} = 333 nm, [**1**] = 5.0×10^{-5} M.

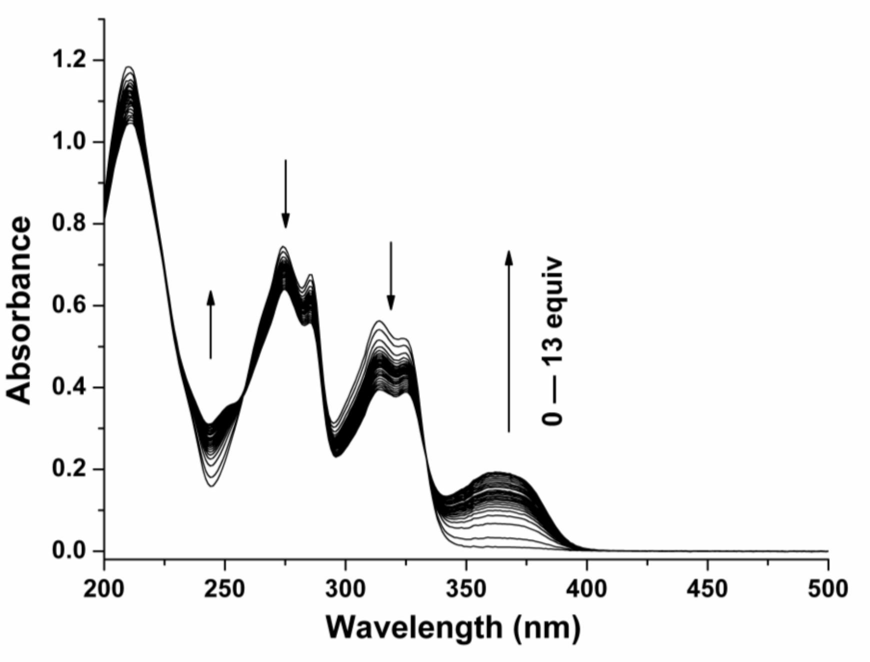

Fig. S7 Absorption spectra of **1** in acetonitrile with the increase of $Mg(ClO_4)_2$. [**1**] = 5.0×10^{-5} M.

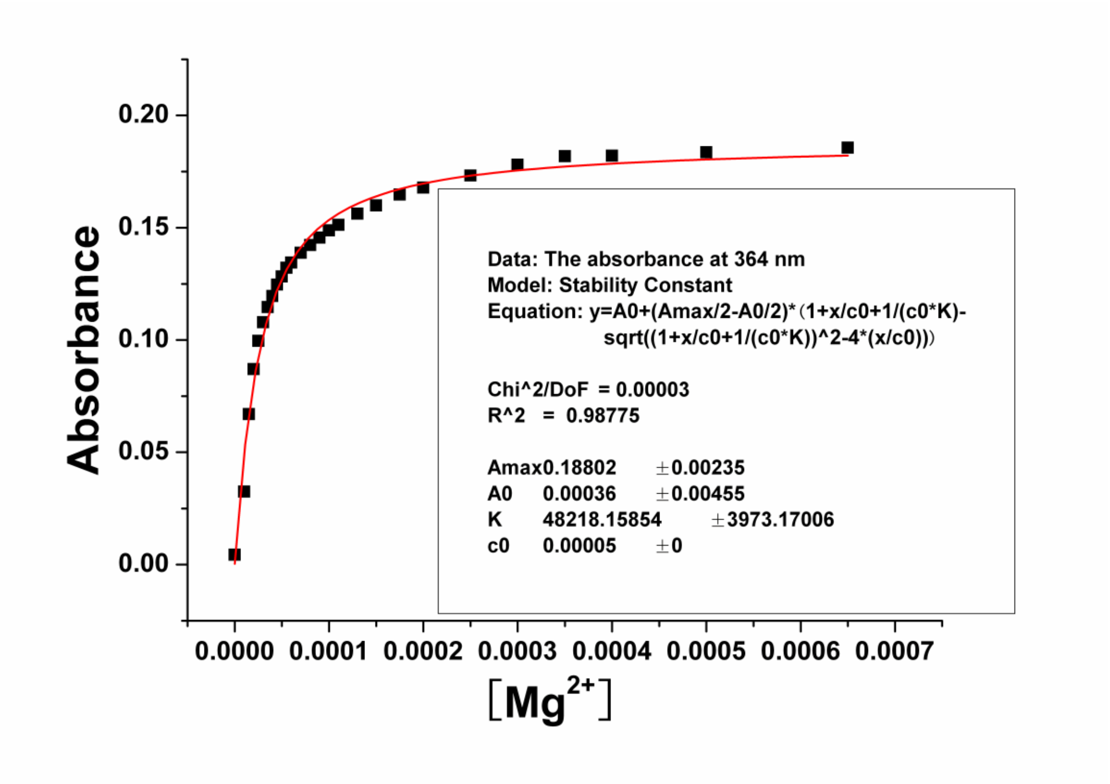

Fig. S8 The absorbance change of **1** at 364 nm in acetonitrile with the increase of $Mg(ClO_4)_2$. The red line is the nonlinear fitting curve obtained assuming a 1:1 association between **1** and Mg^{2+}. The association constant was estimated to be 4.8 (± 0.4) × 10^4 M^{-1}. [**1**] = 5.0 × 10^{-5} M.

4. Effect of water content on the fluorescence response of 1 and its complexes.

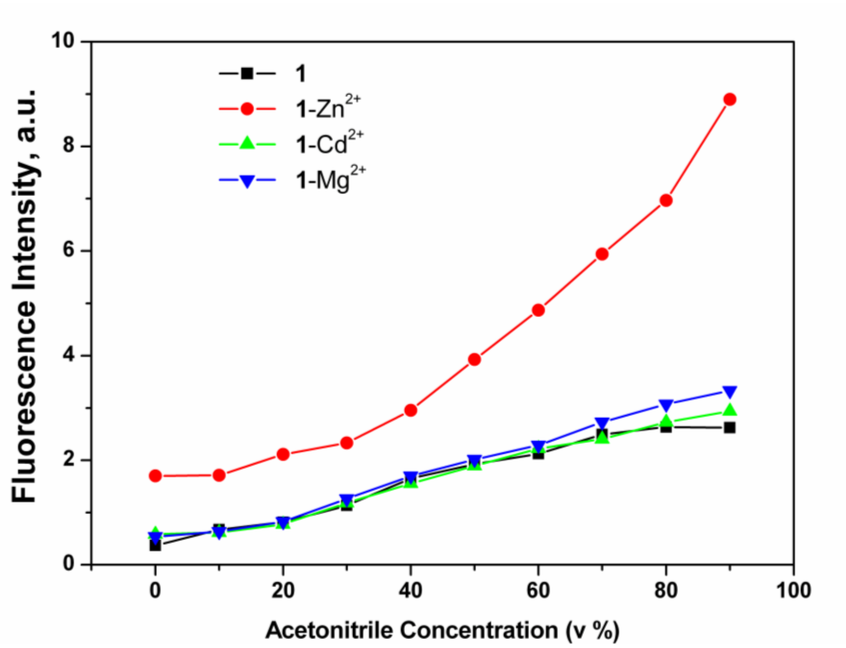

Fig. S9 Effect of water content on the fluorescence intensity of **1** (50 μM) in the presence of Zn^{2+}, Cd^{2+} and Mg^{2+} ions (5 equiv) in CH_3CN/H_2O binary solvent mixture. The λ_{max}em are 410 nm for **1**, 432 nm for **1**-Zn^{2+} system, 415 nm for **1**-Mg^{2+} system and 413 nm for **1**-Cd^{2+} system, respectively. λ_{ex} = 333 nm.

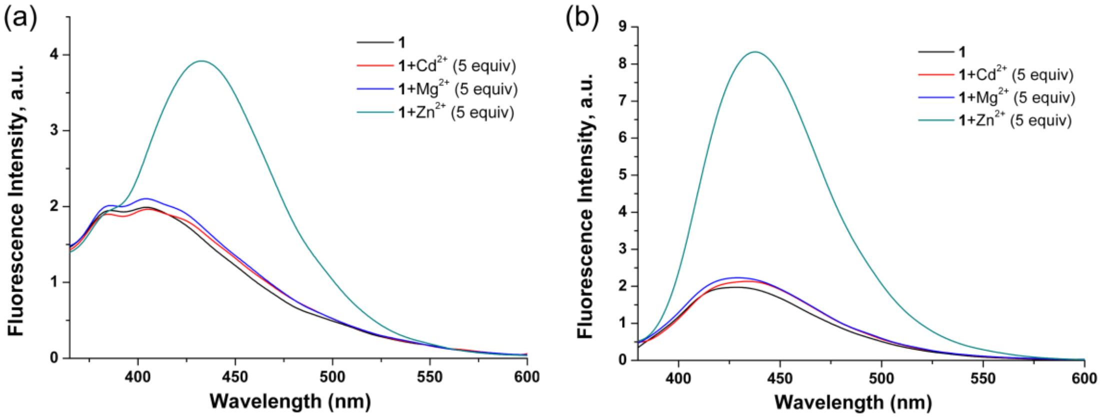

Fig. S10 Fluorescence spectra of **1** (50 μM) in the presence of Zn^{2+}, Cd^{2+} and Mg^{2+} ions (5 equiv) in 1:1 CH_3CN/H_2O binary solvent mixture. (a) λ_{ex} = 333 nm; (b) λ_{max}ex = 363 nm.

5. Absorption titration of 1 with Zn^{2+}, Cd^{2+} and Mg^{2+} in 1:1 CH_3CN/H_2O.

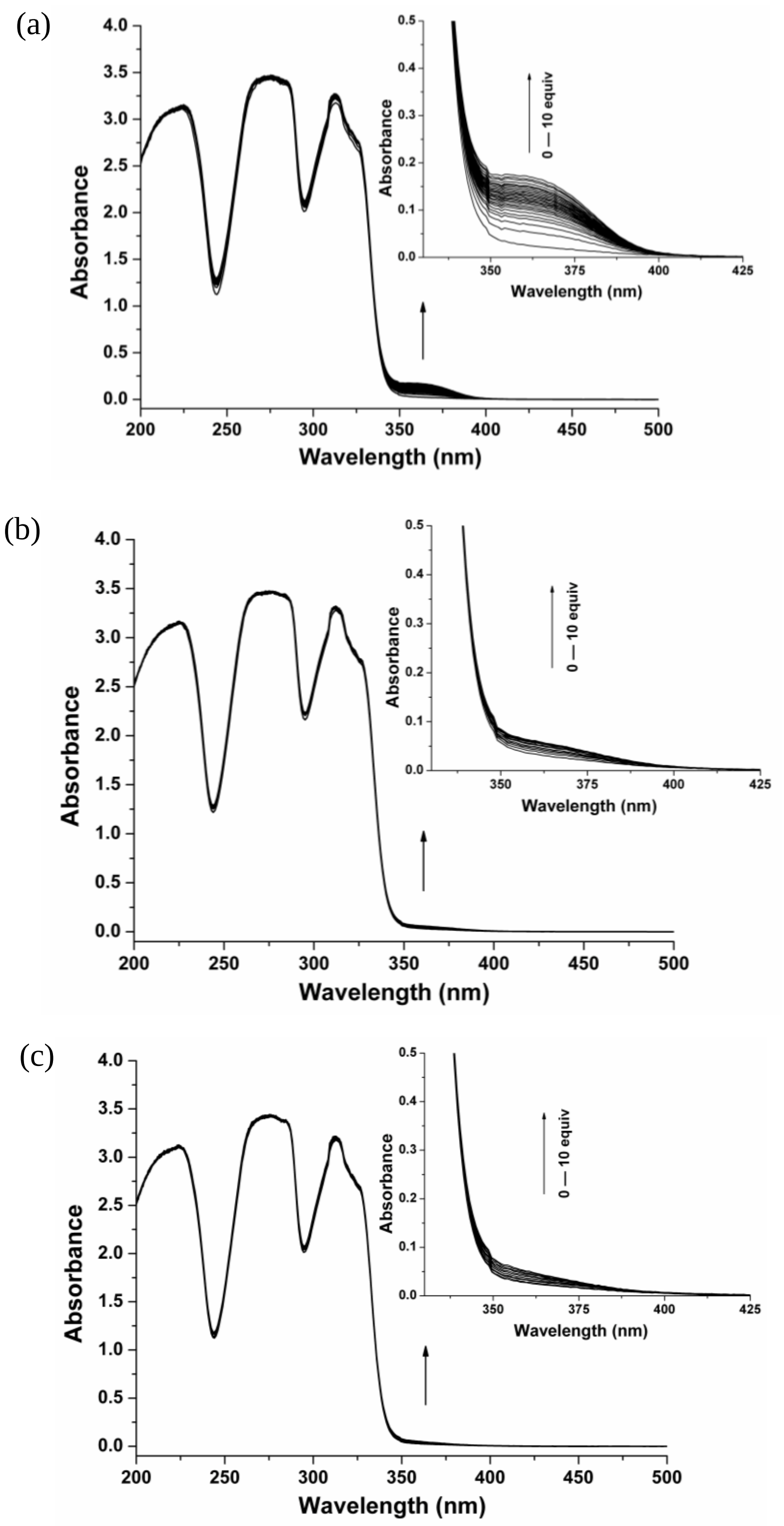

Fig. S11 Absorption spectra of **1** in 1:1 CH_3CN/H_2O binary solvent mixture with the increase of $Zn(ClO_4)_2$ (a), $Cd(ClO_4)_2$ (b) and $Mg(ClO_4)_2$ (c). [**1**] = 5.0×10^{-4} M.

6. Effect of the pH on the fluorescence intensity of 1 and 1-Zn^{2+} in CH_3CN-H_2O mixed solvent.

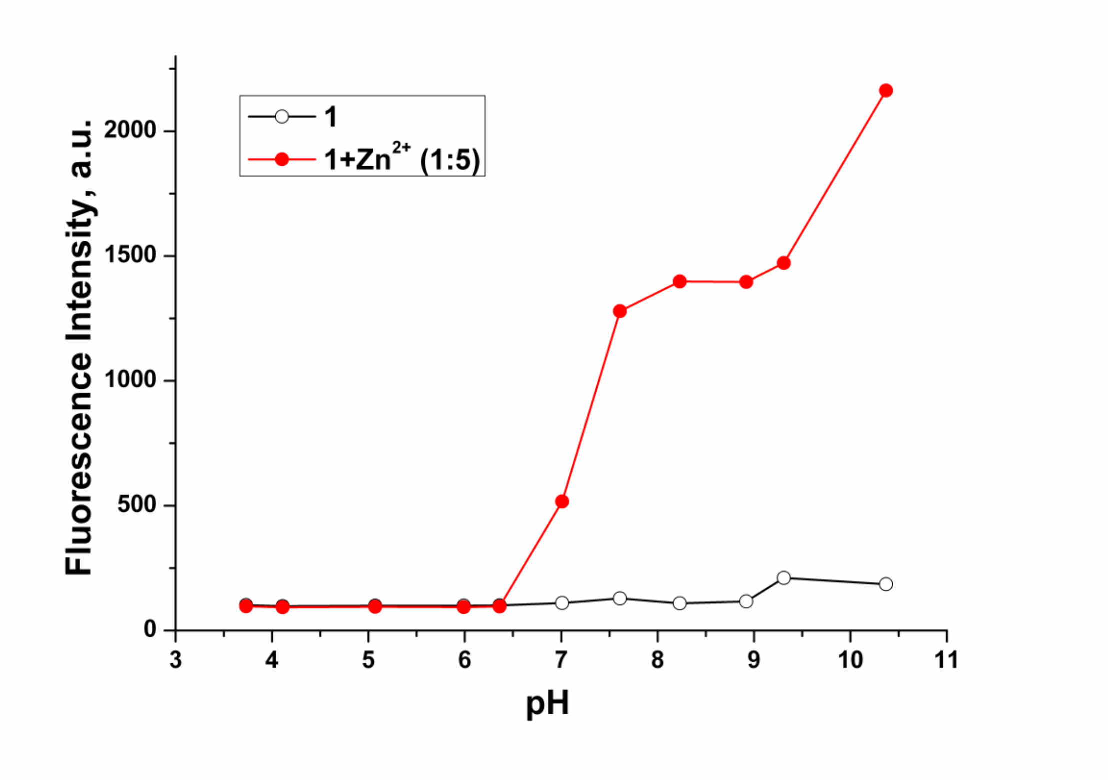

Fig. S12 Effect of the pH on the fluorescence intensity of **1** and **1** in the presence of Zn^{2+}. The λ_{max}em are 437 nm for **1**-Zn^{2+} system and 420 nm for **1**. λ_{max}ex = 363 nm, [**1**] = 5.0 × 10^{-5} M.

7. The detection limit (LOD) and association constant of 1-Zn^{2+} in HEPES buffer.

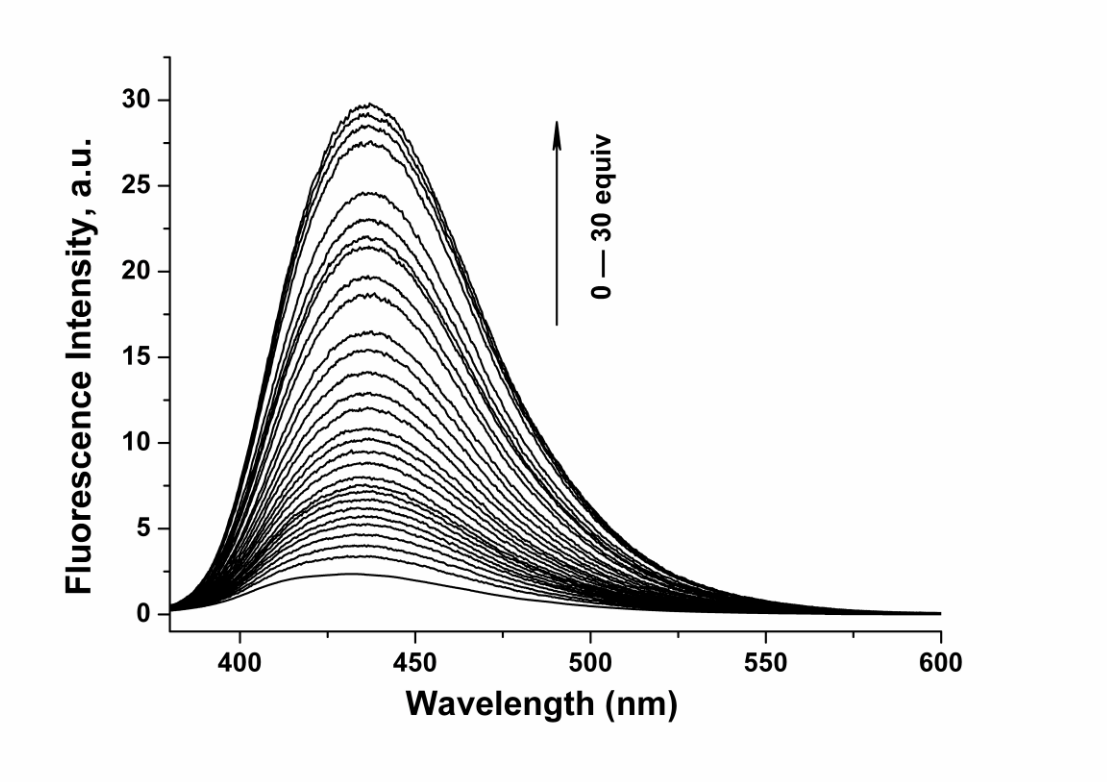

Fig. S13 Fluorescence spectra of **1** in HEPES buffer (10 mM, pH = 7.2, CH_3CN/H_2O = 1:1, v/v) in the presence of increasing concentration of $Zn(ClO_4)_2$. $\lambda_{max}ex$ = 363 nm, [**1**] = 5.0×10^{-5} M.

8. Photo showing in natural light and fluorescence changes.

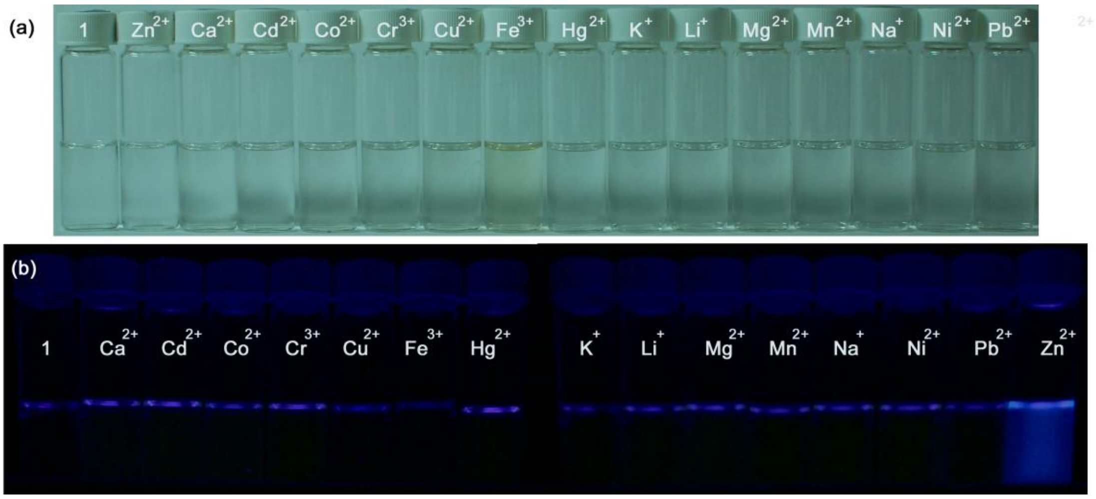

Fig. S14 Photo showing in natural light (a) and fluorescence changes (b) of **1** (10 μM) in the presence of various metal ions (50 μM) in aqueous acetonitrile solution (50 %). λ_{ex} = 365 nm

9. Time-resolved fluorescence decay, radiative rate and the total nonradiative rate data.

Table S1 Radiative and the total nonradiative rate data.

	τ_i (ns)	c$_i$ (%)	α_i	τ_f (ns) (average)	Φ_f	k_r (s^{-1})	k_{nr} (s^{-1})	χ^2
1	0.33	30.47	0.166	3.20	0.123	3.84×10^7	2.74×10^8	1.077
	2.24	35.60	0.028					
	6.77	33.93	0.009					
1+Zn^{2+} mol ratio (1:5)	2.52	13.68	0.003	3.99	0.542	1.36×10^8	1.15×10^8	0.962
	4.19	86.32	0.013					

τ_i is the decay time of the component i; c$_i$ is the relative content of the component i; α_i is the pre-exponential factor or amplitude of the component i; τ_f is the intensity-averaged decay time (or lifetime) of the molecule; Φ_f is the fluorescence quantum yield of the compound; k_r and k_{nr} are the radiative rate constant and the total nonradiative rate constant, respectively; χ^2 is the goodness-of-fit value of fitting curve.

The mean fluorescence lifetime is calculated by using the following formula:

$$\tau_f = \frac{\sum_i \alpha_i \tau_i^2}{\sum_i \alpha_i \tau_i}$$

10. Theoretical modelling

The geometry optimizations were performed in vacuum using the hybrid density functional Becke-3-Lee-Yang-Parr (B3LYP) potential in conjuration with a 6-31G basis set for the H, C, N, O atoms, and a LANL2DZ effective core potential (ECP) basis set for the Zn atom, as implemented in GAUSSIAN 09 software package. This level is often estimated to be adequate for the geometry optimization of aromatic compounds with metal interactions. Harmonic vibrations were also calculated for the obtained structure to establish that a true minimum was reached.

Table S2 The data are in the table below:

COMPND								
HETATM	1	C	UNK	0	-0.152	0.884	-0.570	C
HETATM	2	C	UNK	0	-0.152	2.315	-0.570	C
HETATM	3	C	UNK	0	3.709	4.228	-0.570	C
HETATM	4	C	UNK	0	-1.389	3.035	-0.613	C
HETATM	5	C	UNK	0	2.608	5.948	-2.033	C
HETATM	6	C	UNK	0	1.095	2.988	-0.592	C
HETATM	7	C	UNK	0	1.155	4.369	-0.691	C
HETATM	8	C	UNK	0	-3.419	5.394	0.360	C
HETATM	9	C	UNK	0	-2.278	6.770	-1.387	C
HETATM	10	C	UNK	0	-1.336	4.455	-0.790	C
HETATM	11	C	UNK	0	-3.529	4.726	-2.081	C
HETATM	12	C	UNK	0	-0.075	5.059	-0.808	C
HETATM	13	C	UNK	0	0.703	-1.171	-0.682	C
HETATM	14	C	UNK	0	2.200	-6.655	-3.789	C
HETATM	15	C	UNK	0	-2.616	5.315	-0.968	C
HETATM	16	C	UNK	0	2.481	5.158	-0.701	C
HETATM	17	C	UNK	0	3.084	-1.737	-0.758	C
HETATM	18	C	UNK	0	1.283	-3.516	-0.739	C
HETATM	19	C	UNK	0	3.856	-1.830	0.551	C
HETATM	20	C	UNK	0	1.277	-4.029	-2.173	C
HETATM	21	C	UNK	0	3.543	-2.058	3.745	C
HETATM	22	C	UNK	0	0.840	-6.035	-3.517	C
HETATM	23	C	UNK	0	4.069	-3.015	2.687	C
HETATM	24	C	UNK	0	2.495	6.154	0.492	C
HETATM	25	H	UNK	0	-2.789	5.773	1.173	H
HETATM	26	H	UNK	0	3.546	6.515	-2.044	H
HETATM	27	H	UNK	0	1.787	6.660	-2.166	H

HETATM	28	H	UNK	0	2.610	5.268	-2.892	H
HETATM	29	H	UNK	0	4.624	4.830	-0.570	H
HETATM	30	H	UNK	0	3.778	3.525	-1.408	H
HETATM	31	H	UNK	0	3.688	3.656	0.365	H
HETATM	32	H	UNK	0	2.426	5.621	1.447	H
HETATM	33	H	UNK	0	1.663	6.865	0.439	H
HETATM	34	H	UNK	0	-3.819	4.419	0.644	H
HETATM	35	H	UNK	0	1.997	2.395	-0.537	H
HETATM	36	H	UNK	0	-0.028	6.132	-0.926	H
HETATM	37	H	UNK	0	3.179	-0.715	-1.123	H
HETATM	38	H	UNK	0	3.561	-2.389	-1.499	H
HETATM	39	H	UNK	0	0.293	-3.653	-0.296	H
HETATM	40	H	UNK	0	1.988	-4.096	-0.139	H
HETATM	41	H	UNK	0	5.139	-2.885	2.513	H
HETATM	42	H	UNK	0	3.847	-4.057	2.916	H
HETATM	43	H	UNK	0	0.554	-5.318	-4.290	H
HETATM	44	H	UNK	0	0.058	-6.783	-3.386	H
HETATM	45	H	UNK	0	4.009	-2.289	4.709	H
HETATM	46	H	UNK	0	2.459	-2.156	3.857	H
HETATM	47	H	UNK	0	3.785	-1.022	3.492	H
HETATM	48	H	UNK	0	2.155	-7.249	-4.709	H
HETATM	49	H	UNK	0	2.500	-7.317	-2.971	H
HETATM	50	H	UNK	0	2.964	-5.884	-3.923	H
HETATM	51	H	UNK	0	-4.357	5.413	-2.290	H
HETATM	52	H	UNK	0	-3.955	3.776	-1.748	H
HETATM	53	H	UNK	0	-2.964	4.588	-3.013	H
HETATM	54	H	UNK	0	-3.210	7.317	-1.558	H
HETATM	55	H	UNK	0	-1.695	6.804	-2.314	H
HETATM	56	H	UNK	0	-1.726	7.307	-0.608	H
HETATM	57	H	UNK	0	-4.267	6.080	0.243	H
HETATM	58	H	UNK	0	3.427	6.731	0.489	H
HETATM	59	H	UNK	0	-3.273	2.502	1.024	H
HETATM	60	H	UNK	0	-4.102	0.821	-3.596	H
HETATM	61	H	UNK	0	-3.727	2.207	-2.830	H
HETATM	62	H	UNK	0	-3.743	-2.267	-1.862	H
HETATM	63	H	UNK	0	-2.199	-1.898	-1.403	H
HETATM	64	H	UNK	0	-4.499	1.006	1.145	H
HETATM	65	H	UNK	0	-5.139	-0.489	0.634	H
HETATM	66	H	UNK	0	-4.082	2.809	2.456	H
HETATM	67	N	UNK	0	-0.611	-1.314	-0.773	N
HETATM	68	N	UNK	0	-1.140	0.016	-0.674	N
HETATM	69	N	UNK	0	1.665	-2.106	-0.671	N
HETATM	70	O	UNK	0	4.852	-1.144	0.784	O
HETATM	71	O	UNK	0	0.843	-5.317	-2.204	O

HETATM	72	O	UNK	0	-3.122	-1.570	-1.600	O
HETATM	73	O	UNK	0	-2.574	2.384	-0.477	O
HETATM	74	O	UNK	0	1.631	-3.372	-3.157	O
HETATM	75	O	UNK	0	-3.792	1.235	-2.775	O
HETATM	76	O	UNK	0	3.366	-2.798	1.382	O
HETATM	77	O	UNK	0	-4.579	0.270	0.417	O
HETATM	78	O	UNK	0	-3.878	2.173	1.757	O
HETATM	79	O	UNK	0	1.068	0.171	-0.552	O
HETATM	80	ZN	UNK	0	-3.140	0.459	-0.970	Zn

References:

Gaussian 09, Revision A.02, M. J. Frisch, G. W. Trucks, H. B. Schlegel, G. E. Scuseria, M. A. Robb, J. R. Cheeseman, G. Scalmani, V. Barone, B. Mennucci, G. A. Petersson, H. Nakatsuji, M. Caricato, X. Li, H. P. Hratchian, A. F. Izmaylov, J. Bloino, G. Zheng, J. L. Sonnenberg, M. Hada, M. Ehara, K. Toyota, R. Fukuda, J. Hasegawa, M. Ishida, T. Nakajima, Y. Honda, O. Kitao, H. Nakai, T. Vreven, J. A. Montgomery, Jr., J. E. Peralta, F. Ogliaro, M. Bearpark, J. J. Heyd, E. Brothers, K. N. Kudin, V. N. Staroverov, R. Kobayashi, J. Normand, K. Raghavachari, A. Rendell, J. C. Burant, S. S. Iyengar, J. Tomasi, M. Cossi, N. Rega, J. M. Millam, M. Klene, J. E. Knox, J. B. Cross, V. Bakken, C. Adamo, J. Jaramillo, R. Gomperts, R. E. Stratmann, O. Yazyev, A. J. Austin, R. Cammi, C. Pomelli, J. W. Ochterski, R. L. Martin, K. Morokuma, V. G. Zakrzewski, G. A. Voth, P. Salvador, J. J. Dannenberg, S. Dapprich, A. D. Daniels, Ö. Farkas, J. B. Foresman, J. V. Ortiz, J. Cioslowski, and D. J. Fox, Gaussian, Inc., Wallingford CT, 2009.

11. ^{1}H NMR, ^{13}C NMR and ESI-MS spectra in $CDCl_3$ (*Figure S15-S20)*

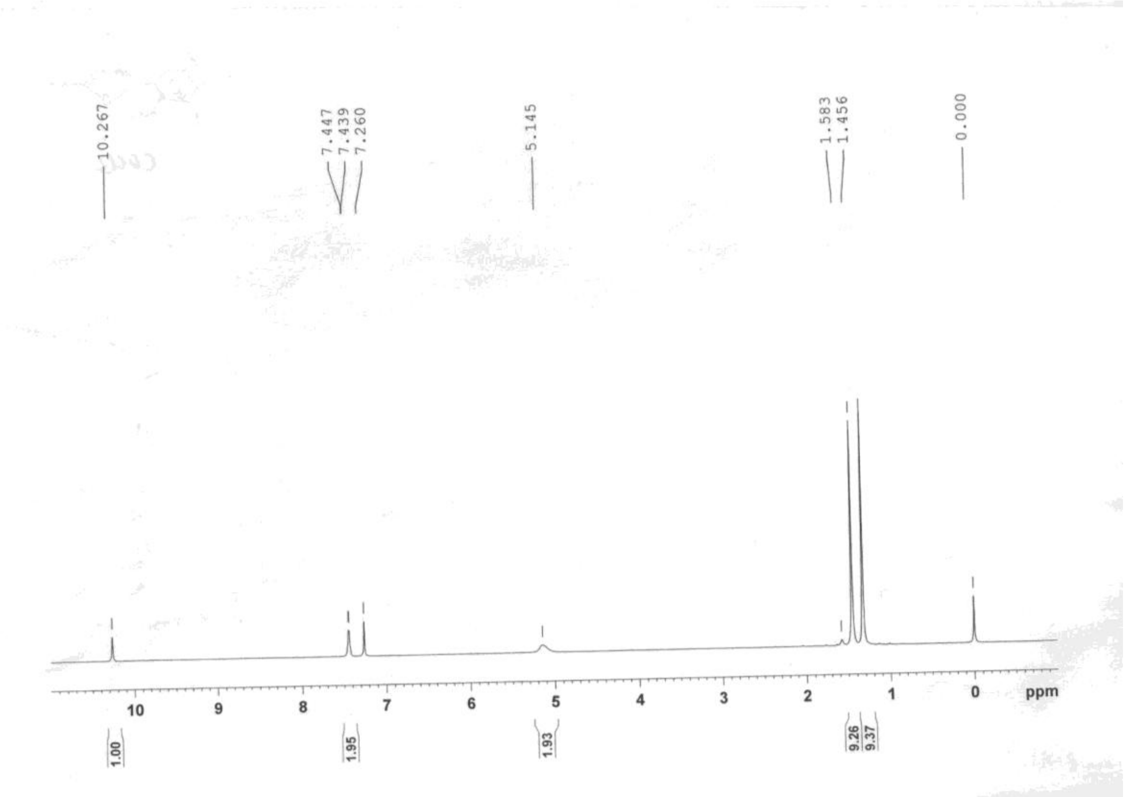

Fig. S15 ^{1}H NMR spectra of **2** in $CDCl_3$

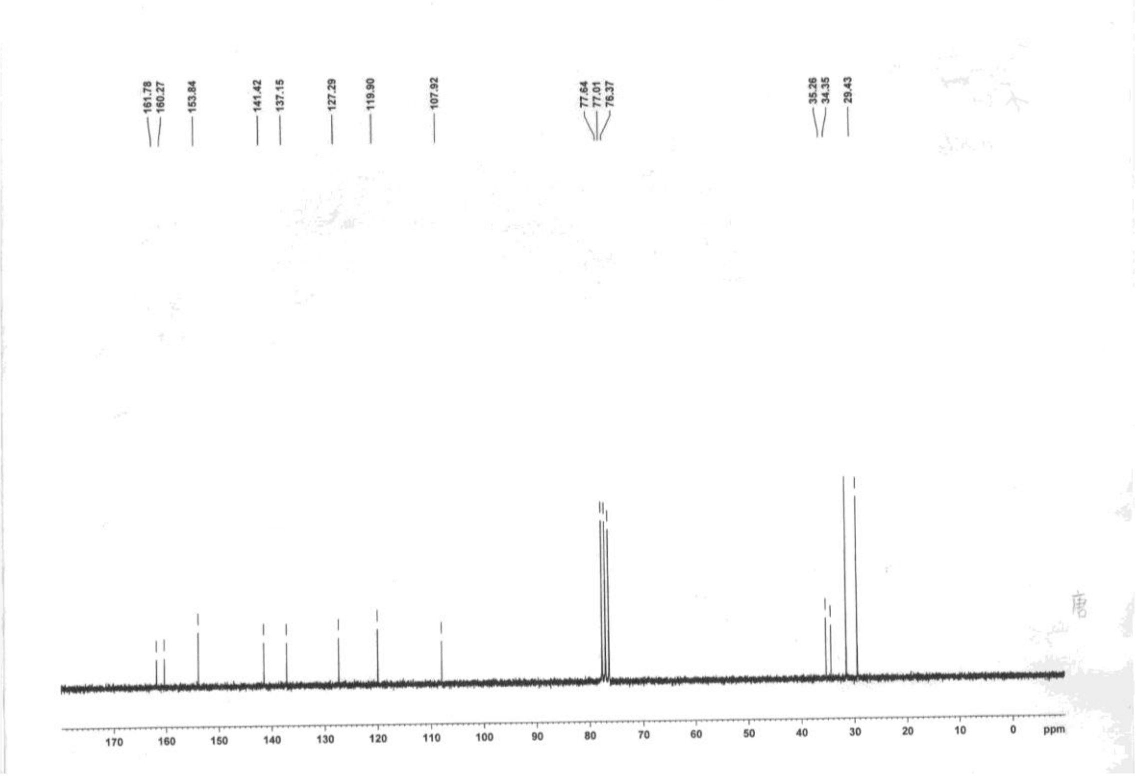

Fig. S16 ^{13}C NMR spectra of **2** in $CDCl_3$

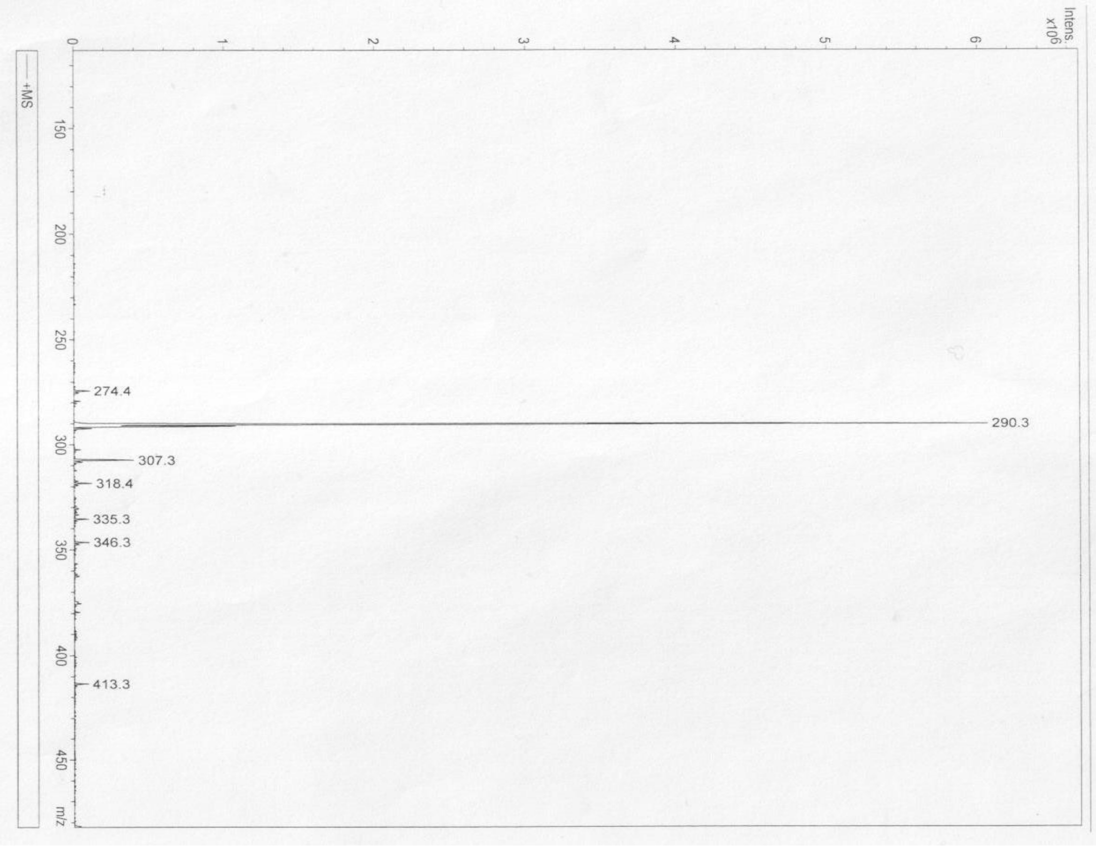

Fig. S17 ESI MS spectra of **2**

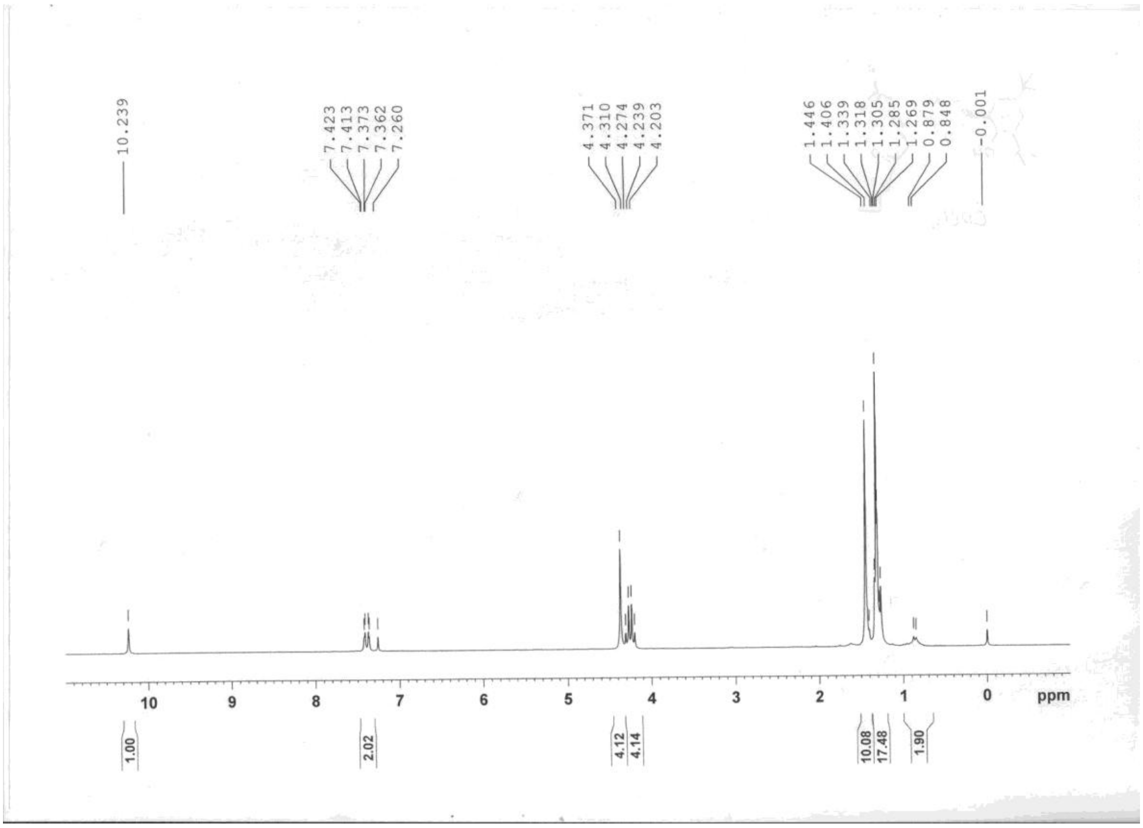

Fig. S18 ^{1}H NMR spectra of **1** in $CDCl_3$

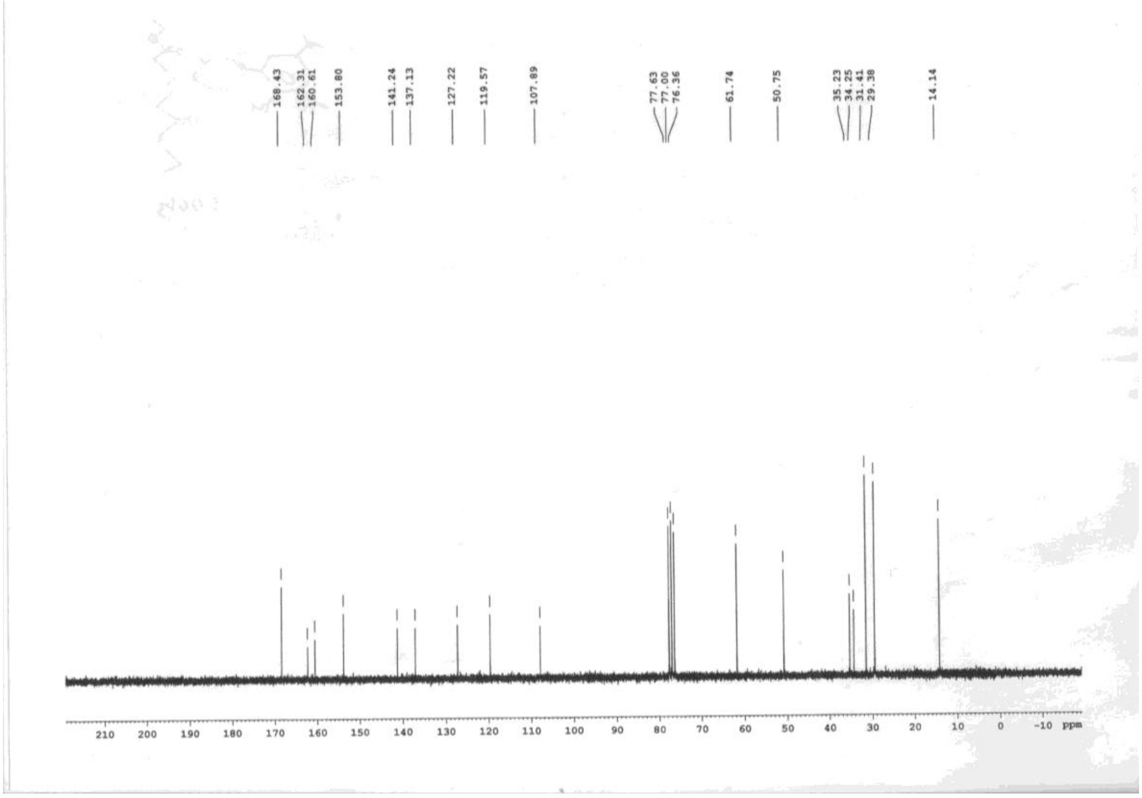

Fig. S19 ^{13}C NMR spectra of **1** in $CDCl_3$

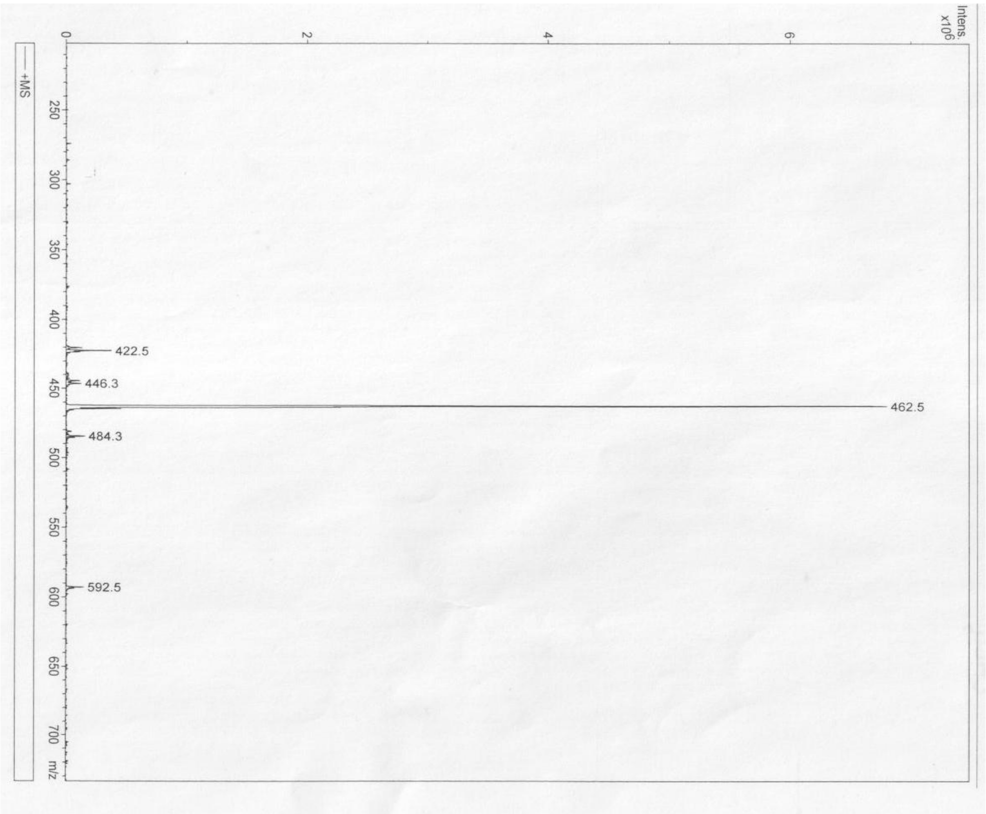

Fig. S20 ESI MS spectra of **1**